

# The Cole Relaxation Frequency as a Parameter to Identify and Spatially Map Cancer in Breast Tissue: Preliminary *In Vivo* Patient Study

William D Gregory<sup>1,2</sup>,  
Shahila Mehboob Christie<sup>1</sup>,  
Christopher W Gregory<sup>1</sup>,  
James J Marx<sup>3</sup>, John Shell<sup>1</sup>  
and Wendy Mikkelson<sup>4</sup>

## Abstract

We have previously reported successful classification of breast cancer vs. benign breast tissue using Cole Relaxation Frequency (CRF) values calculated from impedance measurements on *ex-vivo* breast tissue samples at the time of surgery. Subsequent analysis of outcomes from follow-up medical visits of patients from this cohort provided evidence that the CRF values measured for tissue determined to be cancerous at the time of surgery correlated well with three possible outcomes for the patients (No Recurrence of Cancer; Recurrence with No Metastasis; and Recurrence with Metastasis). We present here data from a small (n=50) IRB approved study to classify and spatially map cancer and benign regions in the breast *in vivo*. Apparatus consisting of two parallel plates mounted on a conventional mammography gantry was used for these measurements. A portion of one of the plates was arranged in a 16 × 16 array of 256 separate regions for measuring the constant voltage impedance sampled at each electrode. Utilizing the patients' pathology and radiology reports we found that the procedure correctly classified benign breast disease or cancer (including invasive and non-invasive ductal or lobular carcinoma) at the location of a suspicious mass, without apparent interference from density of the breast tissue. This approach was shown to be useful for identifying and spatially mapping electrically anomalous regions using the CRF as the classifier.

**Keywords:** Cole relaxation frequency; Breast cancer; Bio-impedance measurements

**Received:** September 02, 2021; **Accepted:** September 16, 2021;

**Published:** September 23, 2021

## Introduction

Electrical Impedance Tomography (EIT) is a technique for creating an image of the interior of an object based on current and voltage measurements acquired by an array of electrodes placed on the outside of the object. Several methods of inverting the externally acquired data to create the internal image have been reported [1]. Unfortunately these methods have poorly conditioned equations connecting the measured data to the internal electrical parameters, producing noise limitations on the output images resulting in discontinuance of an EU funded program in EIT [2].

The work reported here differs from other standard EIT approaches in two significant ways: (a) Placement of the electrodes on the object under test was shown previously to be the source of the poor conditioning of the equations. This problem can be overcome by instead placing the electrodes on a geometric array that allows the inversion solution to be expressed in a complete orthogonal set of equations [3]. Since the poor noise transmission of EIT is caused by inverting a poorly conditioned solution, this work avoids that problem and does not use the electrode placements found in EIT. (b) Furthermore, in this paper we point out that it

is not necessary to invert the equations connecting the external electrode measurements (input data) to the internal electrical properties (output data) to make a 2-D image reflective of the internal electrical parameters of the object. The charges on the external electrodes have sufficient information without inversion to find and classify anomalous regions of breast tissue internal to the breast during real-time *in vivo* measurements.

## Methods

### Apparatus

The apparatus was attached to a standard x-ray mammogram gantry. The device consists of two opposing electrode plates as shown in the Figure 1. The top plate (the Drive plate) is a single electrode of dimensions 26.5 cm × 19.5 cm and is held at 1.0 volts rms at all frequencies. The bottom plate (the Electrode plate) has the same dimensions, but a portion of that plate (10.1 cm × 10.1 cm) is also segmented into a square array of 256 (16 × 16) square regions 6 mm on a side with 0.3 mm spacing between all adjacent

<sup>1</sup>NovaScan Inc., Milwaukee, WI, USA

<sup>2</sup>Professor Emeritus, Colleges of Engineering and Health Sciences, University of Wisconsin, Milwaukee, WI, USA

<sup>3</sup>Advocate Aurora Health Care, Milwaukee, WI, USA (retired)

<sup>4</sup>Director, Advocate Aurora St. Luke's Comprehensive Breast Health Center, Milwaukee, WI, USA

**Corresponding author:** William D Gregory, Colleges of Engineering and Health Sciences, University of Wisconsin, Milwaukee, USA, E-mail: wgregory@novascanllc.com

**Citation:** Gregory WD, Christie SM, Gregory CW, Marx JJ, Shell J, et al. (2021) The Cole Relaxation Frequency as a Parameter to Identify and Spatially Map Cancer in Breast Tissue: Preliminary *In Vivo* Patient Study. *Transl Biomed* Vol.12 No.9:192

metal (circled region in Figure 1B, also shown in a close-up view in Figure 1C). All regions of the electrode plates are held at 0 volt rms at all frequencies. These electrodes allow the current flowing to and from the plate to be separately measured at each position on the electrode array. Both plates have a platinum surface that has been further coated by rapid electrochemical deposition of more platinum to produce a molecular-scale rough surface caused by uneven deposition of the extra platinum.

### Clinical data acquisition

A member of the study team temporarily modifies a standard mammography gantry system by removing the top compression plate of the device and replacing it with the Drive Plate of the apparatus. The Electrode Plate (containing the 256-sensor array of current electrodes) then replaces the film or digital x-ray detector package of the mammography unit as shown in Figure 1 (A,B). Referencing the patient's diagnostic mammogram, MRI,

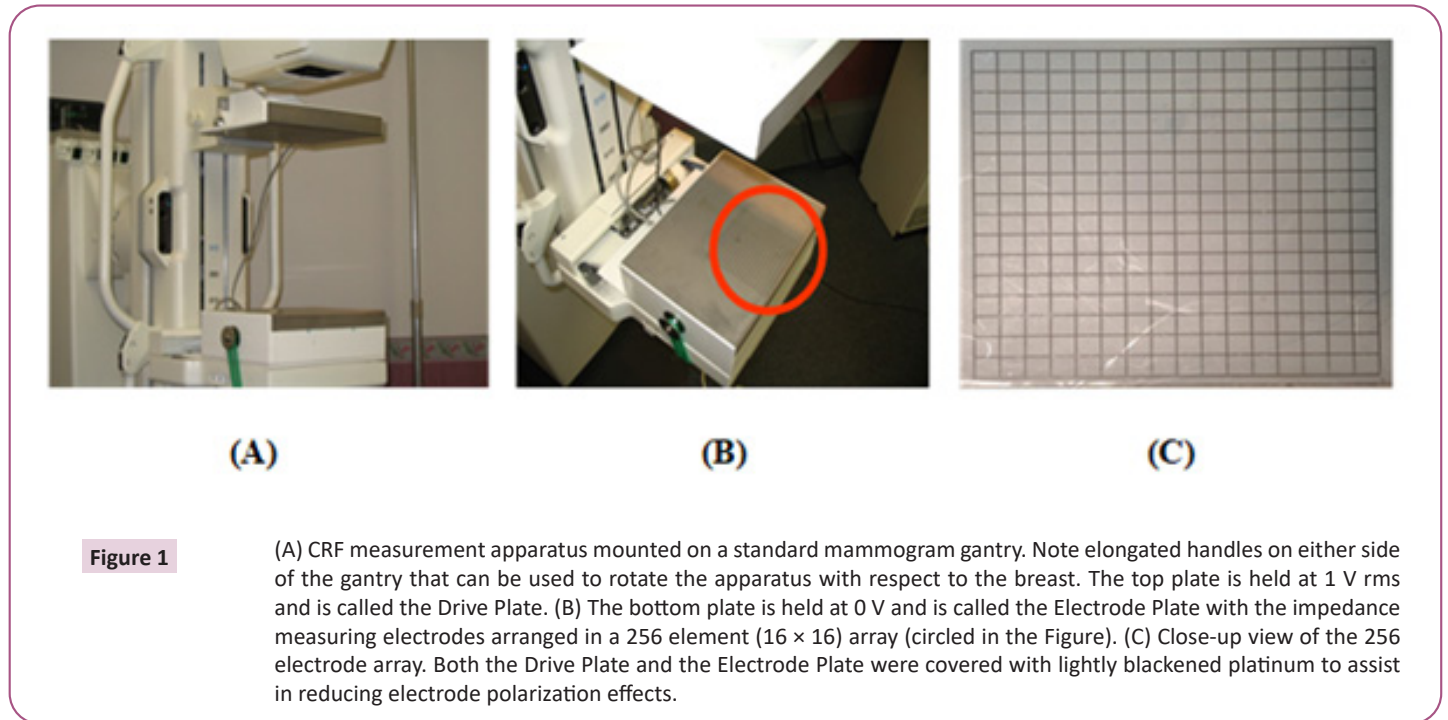


**Figure 1**

(A) CRF measurement apparatus mounted on a standard mammogram gantry. Note elongated handles on either side of the gantry that can be used to rotate the apparatus with respect to the breast. The top plate is held at 1 V rms and is called the Drive Plate. (B) The bottom plate is held at 0 V and is called the Electrode Plate with the impedance measuring electrodes arranged in a 256 element (16 × 16) array (circled in the Figure). (C) Close-up view of the 256 electrode array. Both the Drive Plate and the Electrode Plate were covered with lightly blackened platinum to assist in reducing electrode polarization effects.

ultrasound or other modality of lesion orientation information, a clinical technologist positions the breast so that the suspect lesion/tumor is properly oriented over the 16 × 16 sensor array and then proceeds to center and compress the patient's breast between the plates. A conducting gel is used to ensure contact between the electrodes and the breast, as is common in electrocardiography.

Four total scans per breast are taken in four different orientations by rotating the gantry 180 degrees after the first scan, then by 90 degrees after the second scan, and lastly another 180 degrees after the third scan for the fourth and final scan. Each scan of 9 logarithmically spaced frequencies (ranging from  $1 \times 10^4$  to  $1 \times 10^6$  Hz) with 256 samples per frequency requires about 7 seconds (2304 samples). After acquisition of the data, malignant or benign findings as determined by the device are then compared to pathology findings of the tissue.

### Classification algorithm

We have demonstrated [4-6] that a good method for classifying the health status of breast tissue *ex vivo* is to measure the impedance of the tissue to obtain the Cole relaxation frequency, (CRF or  $f_c$ ) per the Cole model [7].

$$Z_i = \frac{[R(\text{low})_i - R(\text{high})_i]}{[1 + (j(f/f_c))^{\alpha_i}]} + R(\text{high})_i \quad \text{Eq-1}$$

where bold quantities are complex, non-bold are real numbers; the index  $i$  refers to a particular electrode;  $Z_i$  is the complex impedance measured at an electrode; real parameters  $R(\text{low})_i$  and  $R(\text{high})_i$  represent the low and high frequency limits of  $Z_i$ , respectively;  $f$  is the measurement frequency and  $(f_c)$  is the Cole relaxation frequency, both in Hz;  $j = \sqrt{-1}$  and  $\alpha_i$  is a dimensionless number that is inversely related to the broadening in the frequency domain of both the real and the imaginary parts of  $Z$  near the Cole relaxation frequency,  $f_c$ .

The data acquired for this paper were the complex impedances ( $Z_i$ ) measured at each of the 256 electrodes (indexed by the subscript [6]  $i$ ) At a constant rms voltage  $V_0$  (1 volt) applied to the Drive plate, where the impedance measured at each electrode is:

$$Z_i = V_0 / I_i \quad \text{Eq-2}$$

Where  $I_i$  is the current measured at electrode  $i$ .

## Results

We collected four scans per breast in four different orientations similar to the orientations of a mammogram. Each scan is composed of 256 regions (correlating with the 256 sensor array of current electrodes). We have considered two methods for analyzing the data; (a) determine if cancer present in any scan; and (b) to locate suspect regions of a scan.

**Identify presence of cancer in a scan**

We performed an analysis of the data using noise mitigation techniques to allow a physician to concentrate on first evaluating more suspicious scans. An iterative process was developed in MATLAB [8] to analyze the impedance data. A locally weighted robust implementation of the nonparametric Loess smoothing algorithm was applied to each of the  $256 \times 9$  rows of each of the 4 Zi orientation matrices per patient (256 electrodes  $\times$  9 imaginary impedance components of each electrode). The analysis algorithm accepts each row of the  $256 \times 9$  matrix, where each row is fitted to the imaginary component of the Cole function and finding CRF to first eliminate those regions not indicative of malignant tissue. The remaining rows of the matrix that did contain relaxation frequencies in the malignant range were averaged to arrive at a  $1 \times 9$  sample for that orientation. The results are shown in Figure 2 for the patient 13L and for the control patient for each of the 4 gantry orientations. If the CRF identified was within the previously reported frequency range for cancer (CRF >100 kHz)<sup>1</sup> for any of the 4 orientations of the mammogram gantry that breast was classified as CA. If CRF is below 100 kHz then the tissue is classified as Benign (BN).

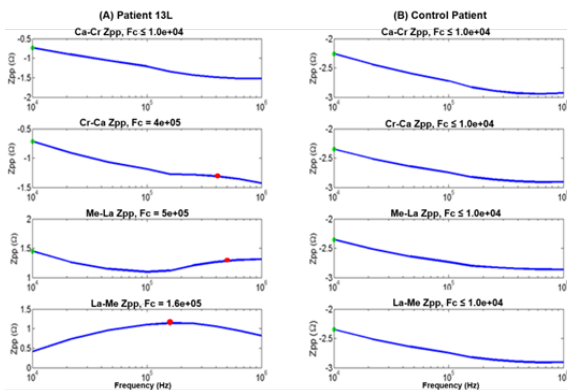


**Figure 2** The Loess smoothed averages of  $-Z_{pp}$  for patient 13L (A) and the control patient (B). The volunteer control patient (not shown in Table 1) is confirmed to be free of any palpable lesions and clear ultrasound and x-ray mammogram. Four different orientations of the positions of the electrode and drive plate are noted. Note that in the Cole eq. 7 it is possible for  $R(\text{low})$  to be greater than or less than  $R(\text{high})$  so  $Z_{pp}$  can be either positive or negative, but in either case  $Z_{pp}$  is a maximum at a peak.

Locate the cancer regions in a scan: Figure 3 displays plots of one scan for each of the two cases presented in Figure 2. Figure 3 (A,B) is a plot of the low frequency (10 kHz) real component ( $Z_p$ ) of the impedance. The value of  $Z_p$  at this (lowest) frequency is a sum of all the Cole curves above that frequency and is a measure of the internal polarization charges at a given position in the specimen.

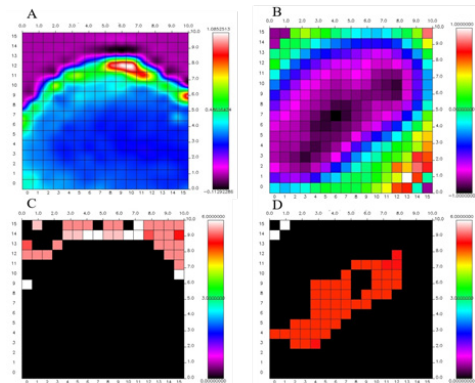


**Figure 3** 256 electrode image of one scan for control patient (A,C) and patient 13L (B,D). (A,C) is a plot of the real component of the impedance at 10 kHz that allows an estimate of where the breast boundary is located. (B,D) is a plot of the  $\log_{10}(f_c)$ . For the control patient all electrodes register a non-cancer  $f_c$  (C) while for patient 13L the cancerous region is highlighted in red in (D). Note that the color bar is different for the impedance and  $f_c$  plots: It ranges from minimum to maximum impedance in (A,B) and 0 to 6 for the  $\log_{10}(f_c)$  plot (C,D).

The value of the impedance changes abruptly at the edge of the breast where the measured current is zero and determines the boundaries of the breast in the images shown in Figure 3 (A,B). Figure 3 (C,D) is a plot of the  $\log_{10}(f_c)$  for each electrode. We note that the control patient had no regions identified as CA internal to the breast while patient 13L had a well-defined region with electrodes having  $f_c$  values in the CA region. These plots are reflective of a breast image highlighting the regions encompassing cancerous cells.

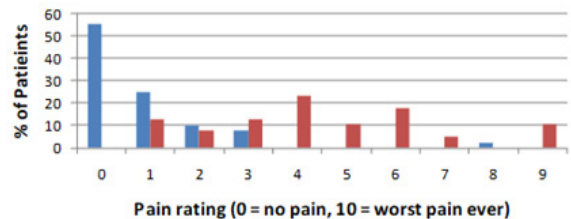


**Figure 4** Histogram reflecting patient pain scale rating of the CRF scans (blue bars) vs. X-ray mammograms (red bars).

**Pathology and radiology results**

Table 1 lists the results of this analysis for the patients participating in this study. Two of the patients had a ‘screen fail’ (due to missing (censored) pathology data). Thus, the total number of patients included in the study was 50.

**Table 1:** Results of analysis for patients in this study. The two screen fails (patients 1 and 39) relate to the absence of pathology data. Pathology report for cases with Cancer (CA) include 21 cases of Ductal Carcinoma *In Situ* (DCIS) and invasive IDC, 3 cases of invasive IDC only, 1 case of DCIS only, 1 case of Lobular Cancer *In Situ* (LCIS) combined with invasive ILC, and 22 benign cases. When needed L and R indicates Left or Right breast for the same patient. <sup>A</sup>: DCIS+ Invasive IDC; <sup>B</sup>: Invasive IDC only; <sup>C</sup>: DCIS only; <sup>D</sup>: LCIS+Invasive ILC; <sup>E</sup>: Information regarding cancer type not available.

Patient #	Pathology Report	<Cole Frequency> BN<100kHz CA>100 kHz	Breast Density	Mass size(mm)	Patient #	Pathology Report	<Cole Frequency> BN<100kHz CA>100 kHz	Breast Density	Mass size(mm)
1	SCREEN FAIL								
2	bn	BN		5	28	bn	BN	Dense	32 months
3	bn	BN			29 <sup>A</sup>	ca	CA	Dense	16
4 <sup>B</sup>	ca	CA		25	30	bn	BN		
5 <sup>C</sup>	ca	CA			31 <sup>A</sup>	ca	CA	CA	60
6	bn	BN		2	32	bn	BN	Dense	10
7 <sup>A</sup>	ca	CA		28	33 <sup>A</sup>	ca	CA	Dense	5
8	bn	BN			34	bn	BN		
9	bn	BN		33	35	ca	CA	Dense	11
10	bn	BN		3	36	bn	BN		
11 <sup>A</sup>	ca	CA		13	37	bn	BN	Dense	
12	bn	BN		5	38	bn	BN	Dense	
13L <sup>A</sup>	ca	CA		6	39	SCREEN FAIL			
13R	bn	BN		30	40 <sup>A</sup>	ca	CA		26
14 <sup>A</sup>	ca	CA	Dense	15	41	bn	BN	Dense	
15	bn	BN			42	bn	BN	Dense	8
16	ca	CA		8	43 <sup>A</sup>	bn	BN		20
17	bn	BN	Dense		44L	ca	CA	Dense	
18 <sup>A</sup>	ca	CA	Dense		44R	ca	CA	Dense	25
19	bn	BN			45	ca	CA		30
20 <sup>A</sup>	ca	CA		8	46 <sup>A</sup>	ca	CA	Dense	23
21	bn	BN	Dense	35	47 <sup>A</sup>	ca	CA		8
22	bn	BN		2	48 <sup>A</sup>	ca	CA		17
23	bn	BN			49 <sup>E</sup>	ca	CA		30
24 <sup>A</sup>	ca	CA	Dense	7	50 <sup>A</sup>	ca	CA		10
25 <sup>A</sup>	ca	CA		17	51 <sup>A</sup>	ca	CA	Dense	38
26 <sup>D</sup>	ca	CA	Dense	20	52 <sup>A</sup>	ca	CA		25
27	bn	BN	Dense						

## Discussion

We have presented an alternative type of mammography that uses the Cole relaxation frequency ( $f(c)$  in Eq-1) as the classifier of the tissue health status. We make the following observations regarding the utility of this method.

### Frequency filtering of BN and CA masses

Breast tissues that are non-cancerous have a relaxation frequency that can differ by one or more orders of magnitude from cancerous regions. This results in a frequency filtering effect that makes it possible to view cancerous regions embedded in non-cancerous tissue, accomplishing the same unmasking effect now possible with 3D mammography without the cost, complexity of the equipment and the health risks associated with x-rays. Additionally, we have also observed that breast density has no effect on the classification method. This is because the

background tissue in the breast (fat and fibrous tissue) have sufficiently different relaxation frequencies from ductal and lobular tissue that they are separable in the frequency domain. .

### Patient Comfort

A survey of the patients was conducted regarding a comparison of the discomfort felt during CRF measurements vs. during a standard x-ray mammogram, based on a scale of 0 for no pain, 9 for extremely painful. We found that over 50% of the patients rated the x-ray mammogram at 5 or above on the pain scale (Figure 4). With our measurements over 50% of patients rated it at 0. This procedure would likely be better received by patients and might help with compliance issues of patients who are deterred by the discomfort of current X-ray mammograms or risk of exposure to radiation.

## Conclusion

The approach presented in this limited study demonstrates excellent results for finding and classifying the health status of breast tissue in-situ, and additionally, being able to map the position of BN or CA regions spatially in the specimen. These promising results will be confirmed by a larger study. The goal of this study was to establish proof of concept that relaxation frequency can be used confirm and classify breast anomalies as BN or CA and also spatially map these anomalies in an in-vivo setting. We now believe that by expanding on these methods it is possible to obtain full 3D images of the anomalies by increasing the number of orientations to localize regions of interest in each viewing plane that intersect the interior of the breast. Thus, this technology can revolutionize breast cancer screening and diagnosis due to ease of use, better sensitivity and safety, and better patient compliance.

## Acknowledgement

This material is based upon work supported in part by the National Science Foundation under Award Numbers: 0944454 and 1058413. Any opinions, findings, and conclusions or recommendations expressed in this publication are those of the authors and do not necessarily reflect the views of the National Science Foundation. In addition, we received support from the University of Wisconsin-Milwaukee; Aurora Health Care Inc.; NovaScan, LLC; the Wisconsin Institute for Biomedical and Healthcare Technologies; and CAMCARE, the research and education foundation of the Charleston Area Medical Center, Charleston, WV. The WiSys subsidiary of the Wisconsin Alumni Research Foundation and the University of Wisconsin System supported a portion of this work. We are grateful to our colleagues at the University of Wisconsin Milwaukee (ShabistanSheerin), Aurora Health Care (Carol Davis and Carol Halliday) and NovaScan

(Paul Voith and Alan Nichols) for their assistance. A special thank you to our advocatusdiaboli, T. Bernstein (consultant and BOD member of NovaScan), for astute observations that materially improved the manuscript of this paper.

## Funding

Research funding has been received from the National Science Foundation, SBIR Phase I #0944454 and Phase IIa and IIb #1058413.

## References

- 1 Webster JG (1990) Electrical impedance tomography: Adam Hilger series on biomedical engineering, Taylor and Francis.
- 2 Barber DC (1996) CAIT (Concerted Action on Impedance Tomography). Preface *Physiol Meas* 17.
- 3 Gregory WD, Gregory CW (2000) Electrical Property Enhanced Tomography (EPET). *Engineering in Medicine and Biology Society, Proceedings of the 22nd International Conference of IEEE* 4: 2632–2635.
- 4 Gregory WD, Marx JJ, Gregory CW, Mikkelsen WM, Tjoe JA, et al. (2012) The Cole relaxation frequency as a parameter to identify cancer in breast tissue. *Med Phys* 39: 4167-4174.
- 5 Shell J, Gregory WD (2017) Efficient cancer detection using multiple neural networks. *IEEE J Transl Eng Health Med* 5:1-7.
- 6 Gregory WD, Christie SC, Shell J, Nahhas GJ, Singh M, et al. (2020) Cole relaxation frequency as a prognostic parameter for breast cancer. *J Patient Cent Res Rev* 7: 343-8.
- 7 Cole KS (1940) Permeability and impermeability of cell membranes for ions. *Cold Spring Harb Symp Quant Biol* 8:110-122.
- 8 <https://www.mathworks.com/products/matlab.html>